International Journal of Scientific Research in Physics and Applied Sciences
Vol.7, Issue.3, pp.22-26, June (2019)
DOI: https://doi.org/10.26438/ijsrpas/v7i3.2226

Research Paper

E-ISSN: 2348-3423

Synthesis and characterization of different percentage (Fe^{2+}) doped copper oxide (CuO) NPs prepared by chemical method

N. Subhalakshmi[1], M. Karunakaran[2]*, K. Kasirajan[3], N.Ganeshwari[4]

[1,2,3,4]Department of Physics, Alagappa Government Arts College, Karaikudi, India- 630003

[*]*Corresponding Author: tvdkaruna@gmail.com, Tel.: +91-8122841591*

Available online at: www.isroset.org

Received: 08/Apr/2019, Accepted: 27/Apr/2019, Online: 30/Jun/2019

Abstract— In the last decade the metal oxide NPs are the promising applications in the research field. The lot of methods to available in the synthesis of NPs, but co-precipitation method is very simple, low cost and environmental friendly. The different percentage (Fe^{2+}) doped copper oxide (CuO) NPs prepared by co-precipitation method. XRD pattern confirms the samples are crystalline in monoclinic structure identified by the JCPDS Card. No (80-0076). The doping concentration increases the crystalline size also decreases. CuO NPs based functional groups are identified from FTIR spectra. UV-Vis Spectroscopy the Fe doped CuO has a band gap is determined in the range of 3.57 to 3.62 eV. The Pl emission spectra revealed a blue shift after introducing Fe into CuO structure, from these studies is better for the preparation of CuO nanoparticles. SEM-the surface morphology of the as prepared CuO nanoparticles has identified by SEM studies the indefinite and closely packed grain is observed. The EDAX spectra showed presence copper, Fe and oxygen atoms.

Keywords— *Co-Precipitation, Doping, Copper Oxide, Structural Studies, Band gap*.

I. INTRODUCTION

The transition metal oxides have been attracting attention due to their physical and chemical properties of the NPs. In the global needs the large production of Copper industry for the last decades increasingly being used for superconducting, semiconducting, thermo electrics, sensors, ceramics, energy storage, antifouling paints, photoconductive and photo thermal applications, including the automotive, ship, and aerospace industries. Oxide-based diluted magnetic semiconductors (DMS) are gaining more attention currently, because of their potential for a spintronic application [1-5]. The metal oxide NPs are the good physical and chemical properties the NPs. The transition metal Oxide NPs such as MnO, CdO, CuO, ZnO, NiO, and TiO_2 for the best optical, magnetic and electrical properties for the Nanostructures numerous applications in the field of catalyst, sensor, fuel cells, drug delivery, electrochemistry and medicine [6-13]. Among the metal oxides NPs, CuO is considered to be one of the most important p-type semiconductors, Non toxic, low cost, abundant, high electrical conductivity.

CuO is with a narrow band gap of about1.2–1.4eV at room temperature .Transition metal oxides Mn, Co. Ni and Cu reveal complicated magnetic as well as electronic structure. Recent investigation shows that the photon property of CuO plays an important role in room-temperature ferromagnetism (RTF). Also, 'Cu' has three oxidation states, Cu^{+}, Cu^{2+}, and Cu^{3+} because of which both hole and electron doping are possible. Cupric oxide CuO is a strongly correlated electron system [14-18].

The doping process is important for altering the properties of the material. Many kinds of material doped in the CuO NPs in previous report, but interesting to dope the transition metal Such as (Mn, Fe, Zn, Ni, and Cd) lot of applications in the field of Magnetic and spintronic. Many kinds of methods available to successfully synthesize Fe doped CuO NPs such as sol–gel, hydrothermal, Microwave irradiation, co-precipitation [19-22]. K.L. Liu et al. A comparative study of the magnetic properties of Fe-doped CuO nanopowders prepared by sol–gel and co-precipitation method. In the two methods for the comparative study both methods are equal contributions of the magnetic behavior [23].

II. MATERIALS AND METHODS

Preparation of Pure and Fe doped CuO NPs:

All the reagents used in this study were of analytical grade obtained from Merck, India and were used as purchased without further purification. Nanocrystalline powders of Fe doped CuO with 2.5, 5, and 7.5 Fe, have been synthesized via co-precipitation method using $ZnCl_2$ and $CuCl_2.2H_2O$ as starting materials. The constituents, in the desired proportion, have been dissolved in distilled water and carefully mixed.

Aq. ammonia has been added slowly to the solution, controlling the pH of the solution within the range 7–8. The resulting precipitates have been collected, thoroughly washed with distilled water, and dried in oven for 3–4 h. The samples were then annealed in Muffle furnace at 500^{o} C for 4 h under normal atmospheric conditions, to improve the crystallinity of samples.

III. RESULTS AND DISCUSSION

X-Ray Diffraction Studies

The characteristic X-ray diffraction patterns of undoped and Fe-doped CuO with varying Fe content were recorded in the range of 2θ between 10° and 80° and shown in Fig. 1(a-d). In the diffraction pattern, all the peaks are well indexed to the monoclinic phase of copper oxide (CuO) that was confirmed from JCPDS card No. 89 – 0076. The diffraction peaks at 2θ = 32.5º, 35.5º, 38.9º, 46.2º, 48.8º, 61.5º, 66.5º and 68.8º are corresponding to the crystal planes of (110), (111), (200), (112), (202), (113), (310) and (221) respectively. No impurities such as Fe metal, Iron oxides or the other phases of Cu_2O and Cu_3O_4 are detected in the XRD pattern, which indicate the purity of the prepared samples. The broad and sharpness of the peaks in the diffraction pattern which indicates the formation of highly crystalline single phase of Fe doped CuO Nanoparticles. These findings indicate that the crystal structure of the base CuO matrix is not distorted by the substitution of Cu^{2+} (0.73Å) ions by Fe^{2+} (0.65Å) ions.

The structural parameters like micro strain, dislocation density, stacking fault probability and texture coefficients were evaluated along with crystallite size using the formula as given under. This parameter can be calculated using Scherer's formula from Full width at half Maximum (FWHM)

$$D = \frac{k\lambda}{\beta Cos\theta} \quad \text{---------- (1)}$$

Where, k is a constant taken to be 0.94, λ is the X-ray wavelength, β is the full-width at half-maximum of the peak and θ is the reflection angle

Where the constant 'k' is the shape factor = 0.94, 'λ' is wavelength of X-rays (1.5406 ÅCuK$_\alpha$) 'θ' is the Bragg's angle and 'β' is FWHM. Dislocations an imperfection in crystal associated with the misregistry of lattice existing in different parts of crystal [14].

$$\delta = \frac{1}{D^2} \quad \text{---------- (2)}$$

The micro strain (ε) developed in thin films can be evaluated from the relation

$$\varepsilon = \left(\frac{\lambda}{DCos\theta} - \beta\right)\frac{1}{\tan\theta} \quad \text{---------- (3)}$$

The stacking fault probability (α) with peak shift Δ (2θ) is given by warren Warekois developed in thin films can be evaluated from the relation

$$\alpha = \frac{2\pi^2}{45\sqrt{3}}\frac{\Delta(2\theta)}{\tan\theta}$$

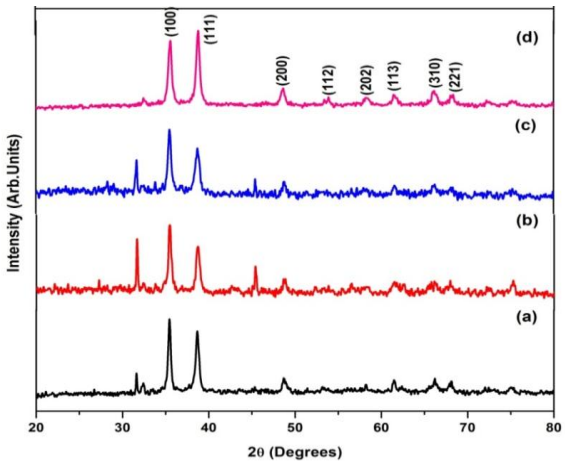

Fig.1. XRD patterns of Fe doped CuO NPs. Fe doping level (a) 0% (b) 2.5%, (c) 5%, and (d) 7.5%

The crystallite size and lattice parameters are calculated using XRD data and are presented in Table 5.1. The average crystallite size of undoped and Fe doped CuO samples are found to be in between the range of 23 to 36 nm. This indicates the crystalline nature of the nanoparticles is slightly decreased with increased Fe content and also the increased microstrain induced the sharpness and intensity of the predominant peaks. This indicates the doping Fe content enhanced the strain of CuO nanoparticles in their positions.

Table – 1: Lattice parameters for Fe doped CuO NPs

Fe doing Level	Lattice parameter (Å)		
	a	b	c
0%	4.676	3.343	5.138
2.5%	4.697	3.358	5.151
5%	4.733	3.367	5.165
7.5%	4.790	3.379	5.189

Table – 2: Micro-structural parameters for Fe doped CuO NPs

Fe doing Level	Crystallite size D (nm)	Dislocation density (δ) $\times 10^{15}$	Micro strain (ε) $\times 10^{-3}$	Stacking fault probability (α)
0%	35.86	1.132	1.166	0.1902
2.5%	32.59	1.214	1.167	0.281
5%	29.45	1.245	1.204	0.259
7.5%	28.66	1.947	1.442	0.448

3.2 Surface Morphological and Element Analysis

Surface Morphological characteristics of the synthesized CuO Nanoparticles samples were examined by scanning electron microscopy technique. Fig. 2 (a) and (b), show the

SEM images of undoped and Fe-doped CuO nanostructures. Fig. 2(b) shows the 5 wt% of Fe doped CuO nano structures. SEM analysis confirms the CuO NPs having uneven shape and the grains are closely packed and there is no any vacancies in the image. The rough and uneven surface is evident is easy to calculate the average size of the Particles around 10-15 nm for undoped and Fe doped CuO respectively. It is evident the small in size particles are highly agglomerated to formed the big grains and 5% doping concentration of Fe, it affects the parent CuO structures.

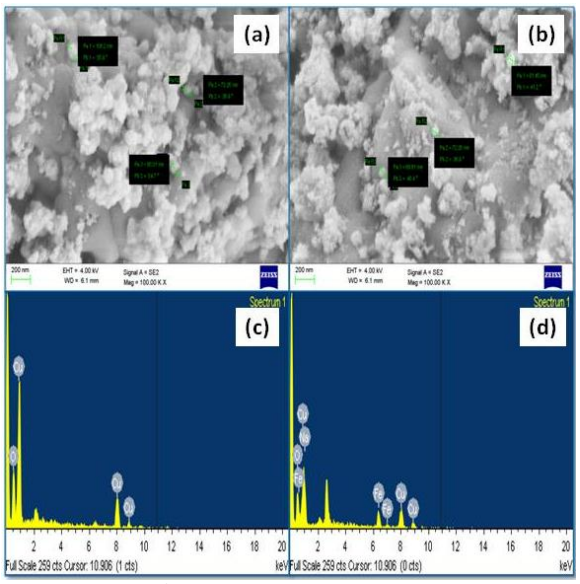

Fig. 2: SEM images of (a) 0% and (b) 5% Fe doped CuO NPs. Fig (c & d) shows the EDAX spectrum

EDAX analysis is used to find out the elemental composition of the prepared Samples. EDAX analysis it is confirmed that presence of copper, oxygen and Iron.

3.3 Functional group analysis

The composition and quality of the Fe doped CuO nano particles are analyzed by FTIR. As shown in Fig.3 sows the CuO Nanoparticles exhibit broad absorption bands between in the range of 500 to 4000 cm^{-1}. The absorption peaks at 517 and may be associated with the characteristic stretching mode of the Cu-O bond and the vibrational Cu-O bond is observed at 780 cm^{-1}, the peak intensity is increased with annealing temperature. This conform that the CuO phase is formed in conformity with XRD data. The absorption peaks at 1384.79 and 1646.67 cm^{-1} is due to the presence of C-H stretching vibration. The medium band at 1647 cm^{-1} to H-O-H indicates the superfluous water molecule absorbed at the surface of the nanoparticles. The absorption band at 3443.09 cm^{-1} has been observed to the existence of OH molecules and 2925.52 cm^{-1} is due to C-H bond stretching.

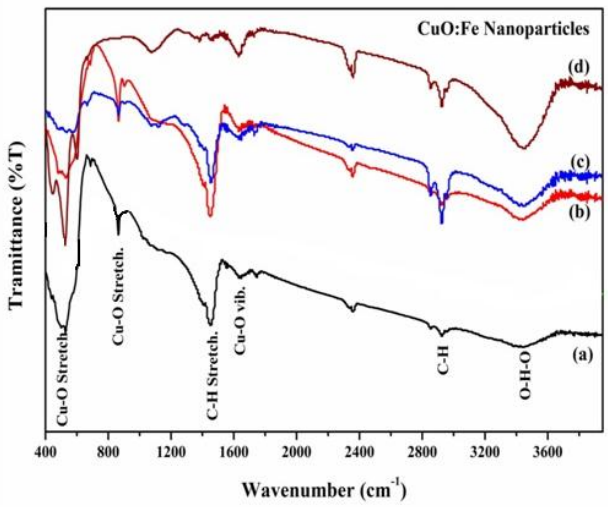

Fig 3: FT-IR spectra for (a) 0%, (b) 2.5%, (c) 5%, and (d) 7.5% Fe doped CuO NPs

3.4 Optical Studies:

3.4.1 UV - Visible Studies:

The optical properties of the pure and Fe-doped CuO nanostructures were studied by UV - Visible - IR spectra. The spectra were recorded between 200 and 1100 nm wavelength region at room temperature. Fig 4 shows the absorbance spectra of Fe doped CuO NPs.

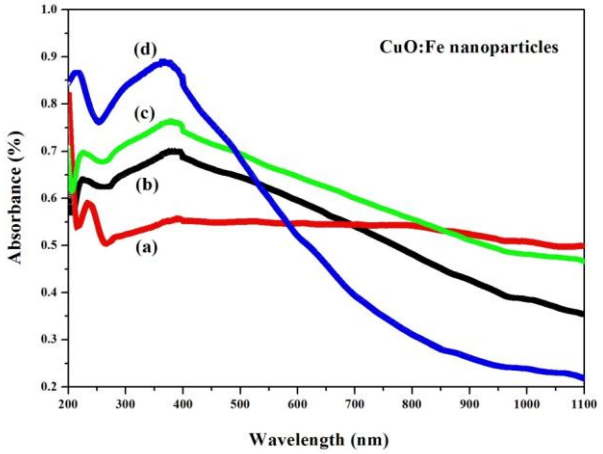

Fig 4: Absorbance spectra for (a) 0%, (b) 2.5%, (c) 5%, and (d) 7.5% Fe doped CuO NPs

The optical gap was calculated by using Tauc relation:

$$(\alpha h\nu) = A\,(h\nu - E_g)^n$$

Where A is a constant, E_g is band gap represents the absorption coefficient, is the photon energy n equals 1/2 and 2 for direct and indirect band gap respectively and by extrapolating the curve in the photon energy axis. The band-gap energy (Eg) values were evaluated by using Tauc's plot as shown in Fig. 5. An obvious blue shift of the absorption edges can also be observed in the Fe-doped CuO system. The direct band gap energy of pure CuO is found to be 2.38 eV

which is in good agreement with the value reported in the literature. The Optical band gap value is increased up to 3.46 eV for 10.0 mol% of Fe, with increasing Fe doping concentration.

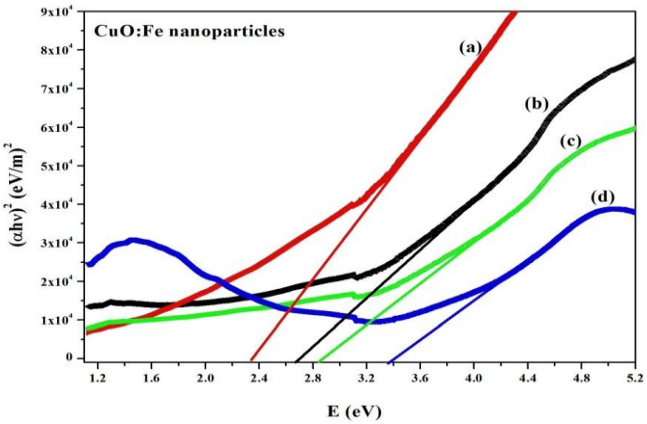

Fig. 5: Tauc plot of (a) 0%, (b) 2.5 % (c) 5 % and (d) 7.5 % Fe doped CuO NPs

3.4.21 Photoluminescence (PL) studies

The room temperature photoluminescence (PL) spectra of the pure as well as Fe-doped CuO samples are shown Fig.6 the peak at 488 nm (blue emission) can be attributed to the transitions of trapped electrons from the donor levels to the valence band [24] The green emission band was observed at 520 and 530 nm in the visible region. The intensity of this PL band increases as the amount of the Fe content increased for 5 and 7.5 mol%. The green emission band reported at 530 nm for deep level defects of CuO. As a result of the recombination of electrons with the holes trapped in singly ionized oxygen vacancies. The band at 530 nm matches well with the above reported emission band of CuO.

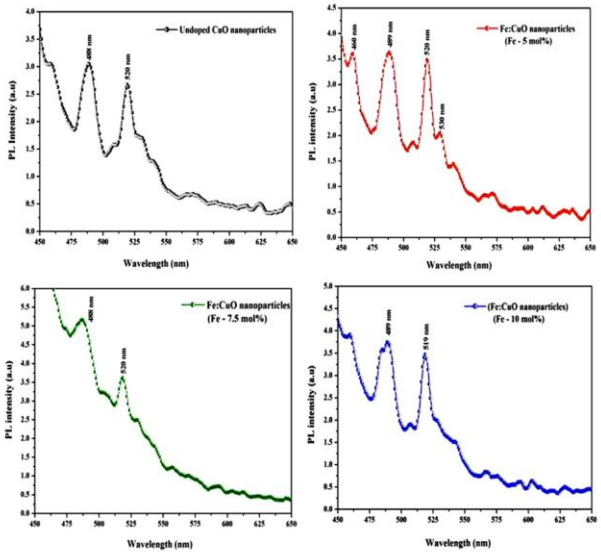

Fig. 6: Photoluminescence spectra of Undoped and Fe doped CuO Nanoparticles

IV. CONCLUSION

In summary, we have studied the effect of Synthesis and characterization of different percentage (Fe^{2+}) doped copper oxide (CuO) NPs prepared by chemical method. X-ray diffraction patterns confirmed the formation of pure CuO monoclinic phase monoclinic phase of copper oxide (CuO) that was confirmed from JCPDS card No. 89 – 0076 with Ni content up to (2.5, 5, and 7.5) wt%, where Ni^{2+} replaces Cu^{2+} ions. SEM analysis having uneven shape and the grains is closely packed and average particle size upto 10-15 nm. The absorption peaks at 517 and may be associated with the characteristic stretching mode of the Cu-O bond. The Optical band gap value is increases up to 3.46 eV for 7.5 % of Fe, with increasing Fe content band gap values increases. The band at 530 nm matches well with the above emission band of CuO NPs.

REFERENCES

[1] Zhu, Jian-fei, and Qi Xiao. *"Meso-macroporous Fe-doped CuO: Synthesis, characterization, and structurally enhanced adsorption and visible-light photocatalytic activity." Journal* of Central South University, Vol. **22,** Issue.**11**, pp **4105-4111, 2015.**

[2] Thangamani, C., Ponnar, M., Priyadharshini, P., Monisha, P., Gomathi, S. S., & Pushpanathan, K. *"Magnetic behavior of Ni-doped CuO nanoparticles synthesized by microwave irradiation method".* Surface Review and Letters, **1850184, 2018**.

[3] Rani, Poonam, Ankita Gupta, Sarabjeet Kaur, Vishal Singh, Sacheen Kumar, and Dinesh Kumar. *"Study of structural and optical properties of Fe doped CuO nanoparticles."* In AIP Conference Proceedings, Vol. **1728,** Issue.**1**, pp **020057, 2016.**

[4] A.A. Oliveira, M.I. Valerio-Cuadros, L.F.S. Tupan, F.F. Ivashita, A. Paesano Jr, *"Size effect on the optical behavior of Fe-doped CuO nanoparticles synthesized by a freeze-drying process"*, Materials Letters Vol. **229,** pp **327-330, 2018.**

[5] Mersian, Hossein, Morteza Alizadeh, and Nahal Hadi. "*Synthesis of zirconium doped copper oxide (CuO) nanoparticles by the Pechini route and investigation of their structural and antibacterial properties."* Ceramics International, Vol. **44,** Issue.**16**, pp **20399-20408, 2018.**

[6] Hoseini Mashhad Toroghi, Asieh Sadat, Nasser Shahtahmassebi, Mahmood Rezaee Roknabadi, Mansour Mashreghi, Elahe Azhir, and Pari Sadat Maddahi. *"Fabrication of CuO: Fe nanoparticles by sol-gel method and study of structural and antibacterial properties."* 2nd conferences on applications of nanotechnology and in sciences, Engineering and medicine, **2011.**

[7] Nasir, Mohd, N. Patra, Md A. Ahmed, D. K. Shukla, Sunil Kumar, D. Bhattacharya, C. L. Prajapat et al. *"Role of compensating Li/Fe incorporation in Cu 0.945 Fe 0.055− x Li x O: structural, vibrational and magnetic properties."* RSC Advances, Vol. **7,** Issue.5**1**, pp **31970-31979, 2017.**

[8] Pugazhendhi, Arivalagan, Smita S. Kumar, M. Manikandan, and Muthupandian Saravanan. *"Photocatalytic and antimicrobial efficacy of Fe doped CuO nanoparticles against the pathogenic bacteria and fungi."* Microbial pathogenesis **2018.**

[9] Layek, Samar, and H. C. Verma. *"Room temperature ferromagnetism in Fe-doped CuO nanoparticles."* Journal of nanoscience and nanotechnology, Vol. **13,** Issue.3, pp **1848-1853, 2013.**

[10] Yang, Z. X., W. Zhong, C. T. Au, X. Du, H. A. Song, X. S. Qi, X. J. Ye, M. H. Xu, and Y. W. Du. *"Novel photoluminescence properties of magnetic Fe/ZnO composites: self-assembled ZnO*

nanospikes on Fe nanoparticles fabricated by hydrothermal method." The Journal of Physical Chemistry, Vol. **C113,** Issue.5**1**, pp **21269-21273, 2009.**

[11] Raksa, Phathaitep, Atcharawan Gardchareon, Torranin Chairuangsri, Pongsri Mangkorntong, Nikorn Mangkorntong, and Supab Choopun. *"Ethanol sensing properties of CuO nanowires prepared by an oxidation reaction."* Ceramics International, Vol. **35,** Issue.2, pp **649-652, 2009.**

[12] Zhang, Qiaobao, Kaili Zhang, Daguo Xu, Guangcheng Yang, Hui Huang, Fude Nie, Chenmin Liu, and Shihe Yang. *"CuO nanostructures: synthesis, characterization, growth mechanisms, fundamental properties, and applications."* Progress in Materials Science, Vol. **60,** pp **208-337, 2014.**

[13] Qiu, Guohong, Saminda Dharmarathna, Yashan Zhang, Naftali Opembe, Hui Huang, and Steven L. Suib. *"Facile microwave-assisted hydrothermal synthesis of CuO nanomaterials and their catalytic and electrochemical properties."* The Journal of Physical Chemistry, Vol. **C116,** Issue.1, pp **468-477, 2011.**

[14] Basith, N. Mohamed, J. Judith Vijaya, L. John Kennedy, and M. Bououdina. *"Structural, optical and room-temperature ferromagnetic properties of Fe-doped CuO nanostructures."* Physica E: Low-dimensional Systems and Nanostructures, Vol. **53,** pp **193-199, 2013.** 53 (2013): 193-199.

[15] Singhal, Sonal, Japinder Kaur, Tsering Namgyal, and Rimi Sharma. *"Cu-doped ZnO nanoparticles: synthesis, structural and electrical properties."* Physica B: Condensed Matter, Vol. 40**7,** Issue.8, pp **31223-1226, 2012.**

[16] Manna, S., and S. K. De. *"Room temperature ferromagnetism in Fe doped CuO nanorods."* Journal of Magnetism and Magnetic Materials, Vol. **322,** Issue.**18**, pp **2749-2753, 2010.**

[17] Naatz, Hendrik, Sijie Lin, Ruibin Li, Wen Jiang, Zhaoxia Ji, Chong Hyun Chang, Jan Köser et al. *"Safe-by-design CuO nanoparticles via Fe-doping, Cu–O bond length variation, and biological assessment in cells and zebrafish embryos."* ACS nano, Vol. **11,** Issue.**1**, pp **501-515, 2017.**

[18] Bhattacharjee, Archita, and M. Ahmaruzzaman. "*CuO nanostructures: facile synthesis and applications for enhanced photodegradation of organic compounds and reduction of p-nitrophenol from aqueous phase."* RSC Advances, Vol. **6,** Issue.47, pp **41348-41367, 2016.**

[19] Ciciliati, Mariani A., Marcela F. Silva, Daniela M. Fernandes, Mauricio AC de Melo, Ana Adelina W. Hechenleitner, and Edgardo AG Pineda. *"Fe-doped ZnO nanoparticles: Synthesis by a modified sol–gel method and characterization."* Materials Letters, Vol. **159,** pp **84-86, 2015.**

[20] Kaur, Jasneet, Jyoti Shah, R. K. Kotnala, and Kuldeep Chand Verma. *"Raman spectra, photoluminescence and ferromagnetism of pure, Co and Fe doped SnO2 nanoparticles."* Ceramics international, Vol. **38,** Issue.**7**, pp **5563-5570, 2012.**

[21] Sun, Peng, Chen Wang, Xin Zhou, Pengfei Cheng, Kengo Shimanoe, Geyu Lu, and Noboru Yamazoe. *"Cu-doped α-Fe2O3 hierarchical microcubes: Synthesis and gas sensing properties.*" Sensors and Actuators B: Chemical, Vol. **193,** pp **616-622, 2014.**

[22] Basith, N. Mohamed, J. Judith Vijaya, L. John Kennedy, and M. Bououdina. *"Structural, morphological, optical, and magnetic properties of Ni-doped CuO nanostructures prepared by a rapid microwave combustion method."* Materials Science in Semiconductor Processing, Vol. 1**7,** pp **110-118, 2014.**

[23] Liu, K. L., S. L. Yuan, H. N. Duan, S. Y. Yin, Z. M. Tian, X. F. Zheng, S. X. Huo, and C. H. Wang. *"A comparative study on the magnetic properties of Fe-doped CuO nanopowders prepared by sol–gel and co-precipitation method."* Materials Letters, Vol.**64,** Issue.2, pp **192-194, 2010.**

[24] Kaiser, Ute, Johannes Biskupek, J. C. Meyer, J. Leschner, Lorenz Lechner, Harald Rose, Michael Stöger-Pollach et al. *"Transmission electron microscopy at 20 kV for imaging and spectroscopy."* Ultramicroscopy, Vol. **111,** Issue.**8**, pp **1239-1246, 2011.**

AUTHORS PROFILE

Dr. M.Karunakaran is currently working as an Assistant Professor in Department of Physics, Alagappa Government Arts College, Karaikudi. He has published more than 50 research papers in reputed international journals and it's also available online. His main research work focuses on Materials Science (Thin films and Nano materials synthesis) He has 13 years of teaching experience and 10 years of research experience.

